Miner Petrol (2013) 107:849–860
DOI 10.1007/s00710-012-0198-6

SPECIAL ISSUE GONDWANA COLLISION

Transpressional regime in southern Arabian Shield: Insights from Wadi Yiba Area, Saudi Arabia

Zakaria Hamimi · Mohamed El-Shafei · Ghazi Kattu · Mohammed Matsah

Received: 9 November 2011 / Accepted: 27 March 2012 / Published online: 17 April 2012

Abstract Detailed field-structural mapping of Neoproterozoic basement rocks exposed in the Wadi Yiba area, southern Arabian Shield, Saudi Arabia illustrates an important episode of late Neoproterozoic transpression in the southern part of the Arabian-Nubian Shield (ANS). This area is dominated by five main basement lithologies: gneisses, metavolcanics, Ablah Group (meta-clastic and marble units) and syn- and post-tectonic granitoids. These rocks were affected by three phases of deformation (D_1–D_3). D_1 formed tight to isoclinal and intrafolial folds (F_1), penetrative foliation (S_1), and mineral lineation (L_1), which resulted from early E-W (to ENE-WSW) shortening. D_2 deformation overprinted D_1 structures and was dominated by transpression and top-to-the-W (−WSW) thrusting as shortening progressed. Stretching lineation trajectories, S-C foliations, asymmetric shear fabrics and related mylonitic foliation, and flat-ramp and duplex geometries further indicate the inferred transport direction. The N- to NNW-orientation of both "in-sequence piggy-back thrusts" and axial planes of minor and major F_2 thrust-related overturned folds also indicates the same D_2 compressional stress trajectories. The Wadi Yiba Shear Zone (WYSZ) formed during D_2 deformation. It is one of several N-S trending brittle-ductile Late Neoproterozoic shear zones in the southern part of the ANS. Shear sense indicators reveal that shearing during D_2 regional-scale transpression was dextral and is consistent with the mega-scale sigmoidal patterns recognized on Landsat images. The shearing led to the formation of the WYSZ and consequent F_2 shear zone-related folds, as well as other unmappable shear zones in the deformed rocks. Emplacement of the syn-tectonic granitoids is likely to have occurred during D_2 transpression and occupied space created during thrust propagation. D_1 and D_2 structures are locally overprinted by mesoscopic- to macroscopic-scale D_3 structures (F_3 folds, and L_3 crenulation lineations and kink bands). F_3 folds are frequently open and have steep to subvertical axial planes and axes that plunge ENE to ESE. This deformation may reflect progressive convergence between East and West Gondwana.

Editorial handling: T. Abu-Alam

Z. Hamimi (✉) · M. El-Shafei · M. Matsah
Department of Structural Geology and Remote Sensing,
Faculty of Earth Sciences, King Abdulaziz University,
Jeddah, Saudi Arabia
e-mail: yahiahamimi@gmail.com

G. Kattu
Saudi Geological Survey,
Jeddah, Saudi Arabia

Introduction

The Arabian-Nubian Shield (ANS) exposed crystalline basement rocks of mostly Neoproterozoic age in northeast Africa and western Arabia as a result of uplift and erosion along the flanks of the Red Sea in Oligocene and younger times (Stern 2002). It represents the northern extension of the East African Orogen (EAO; Stern 1994), or the East African-Antarctic Orogen (EAAO; Jacobs and Thomas 2004), which is a major suture zone separating East and West Gondwana (e.g. Shackleton 1986, 1994, 1996; Muhongo et al. 2003; Johnson and Woldehaimanot 2003; Stern and Johnson 2010). The ANS may be the largest tract of juvenile Neoproterozoic continental crust on Earth (Patchett and Chase 2002).

Neoproterozoic crustal evolution of the ANS has attracted the attention of many workers, and at least four models or paradigms are proposed: 1) infracrustal, 2) Turkic-type, 3) hot-spot, and 4) arc-assembly-orogenic models:

1) Infracrustal model, whereby ophiolites and island-arc volcanics and volcaniclastics were thrusted over an old craton consisting of high- grade gneisses, migmatites and remobilized equivalents during Neoproterozoic time (e.g. Akaad and Noweir 1980; El-Gaby et al. 1988; Abdel-Khalek et al. 1992, 1999; Hamimi et al. 1994; Hamimi 1996; Hamimi and El-Kazzaz 2000; El-Amawy et al. 2000a, b, 2001). The high-grade rocks are suggested to be exposed in several tectonic windows in the ANS forming domal structures or swells, but recent isotopic and geochronologic studies challenge this interpretation (e.g., Liégeois and Stern 2010).
2) Turkic-type orogenic model, whereby much of the ANS formed in broad fore-arc complexes (Sengör and Natal'in 1996).
3) Hot-spot model, whereby much of the ANS is due to accretion of oceanic plateaux formed by upwelling mantle plumes (Stein and Goldstein 1996).
4) Arc assembly (arc accretion) model, whereby EAO juvenile crust was generated around and within a Pacific-sized ocean (Mozambique Ocean). This model was proposed first by Vail (1985) and Stoeser and Camp (1985), and modified by several other workers (e.g., Stern 1994; Stern and Abdelsalam 1998; Stern et al. 2004; Abdelsalam et al. 2003a, b; Abdeen and Abdelghaffar 2011).

The arc assembly model is favored by most ANS researchers. Within the frame of this model, several attempts have been made to classify the northern extension of the EAO (i.e. ANS) into multiple tectonostratigraphic terranes. Amalgamated terranes in the ANS are Halfa, Bayuda, Barka, Hager-Tokar, Ghedem, Haya, Gebeit-Gabgaba, Gerf, Asir, Jeddah, Hijaz, Madyan, Afif and Rayn (Johnson and Woldehaimanot 2003). These terranes contain the initial volcanic and sedimentary deposits that accumulated together with fragments of pre-Neoproterozoic continental crust in the Mozambique Ocean during the rifting of the Rodinian Supercontinent and the re-assembly of cratonic nuclei that would eventually form Gondwana (Johnson 1998). They are separated by ophiolite-decorated intact suture zones and disrupted by shear zones that formed during terminal collision between fragments of East and West Gondwana, beginning about 630 Ma. Tectonic movements along sutures and shear zones range from thrusting to transpression.

Johnson and Woldehaimanot (2003) discussed ANS terrane amalgamation and suture zones, emphasizing the sense of convergence, and identified the following amalgamation (suturing/accretion convergence) events: (1) 786–760 Ma, creating the Bir Umq-Nakasib Suture; the oldest accretionary zone and the longest ophiolite-decorated shear zone in the ANS, (2) 750–660 Ma, creating the Atmur-Delgo and Allaqi-Heiani-Onib-Sol Hamed-Yanbu Sutures, (3) 680–640 Ma, creating the Hulayfah-Ad Dafinah-Ruwah, Halaban and Al Amar Sutures, as well as the Nabitah Fault Zone, (4) 650–600 Ma, creating the Keraf Suture, the youngest arc-arc amalgamation event in the ANS, (5) Post-amalgamation marine basins (e.g. Murdama Basin), epicontinental pull-apart basins, fault-controlled down sags and half grabens (e.g. Hammamat Group of Egypt and Jibalah Group of Arabia), and Late Neoproterozoic structural domes (e.g. Hafafit, Meatiq and El-Shalul of Egypt), (6) Late Neoproterozoic brittle-ductile shears, including N-S trending shears in the southern ANS (Hamisana Shear Zone) and the NW-SE trending Najd system in the northern ANS.

The present work aims at determining the structural setting and tectonic evolution of Neoproterozoic rocks exposed in the Wadi Yiba area in the southwestern Arabian Shield, some 480 km SSE of Jeddah (Fig. 1). The mapped area is ~220 km^2 and is bounded by latitudes 19° 11′ 00″ and 19° 24′ 00″N and longitudes 41° 42′ 00″ and 41° 48′ 00″E. It is known to show most of the structural features and tectonic aspects of the Asir terrane. It has not been previously studied in structural detail. The present study reports results of detailed field structural mapping (scale 1: 40,000) and geometrical analysis of structural fabric data. Special emphasis is given to the deformational history and kinematics of a major high strain zone in the area (WYSZ) and to the temporal and spatial relationships of structural fabrics in the deformed rocks. A model representing the tectonic evolution of the area is proposed, the sequence of deformation is established and the tectonic evolution is interpreted within the frame of existing plate tectonic models for the ANS.

Geologic setting

Based on field relations and observations the Neoproterozoic basement lithologies exposed in the Wadi Yiba area are arranged from oldest to youngest into: gneisses, metavolcanics, ~620–640 Ma Ablah Group, and syn- and post-tectonic granitoids (Fig. 1). These units are traversed by felsic (rhyolitic) to mafic (basaltic) dykes, with variable strikes and strike lengths.

Muscovite-biotite granodiorite gneiss

Gneiss occurs as a narrow, NW-SE trending exposure in the SW part of the mapped area (Fig. 1). This exposure represents a part of an elongated belt extending for about 100 km from the latitude of Al-Qunfedah in the south to the latitude of Al-Darb in the north. The gneiss is grayish-buff to greenish black in color, coarse grained and rich in micas. It is granodioritic orthogneiss, composed of plagioclase (oligoclase), K-feldspars (orthoclase and microcline perthite) and quartz, together with minor muscovite and biotite. Opaques, zircon, sphene and apatite are accessories, whereas epidote and kaolinite are secondary minerals, reflecting greenschist-facies metamorphism. Samples collected near the lower

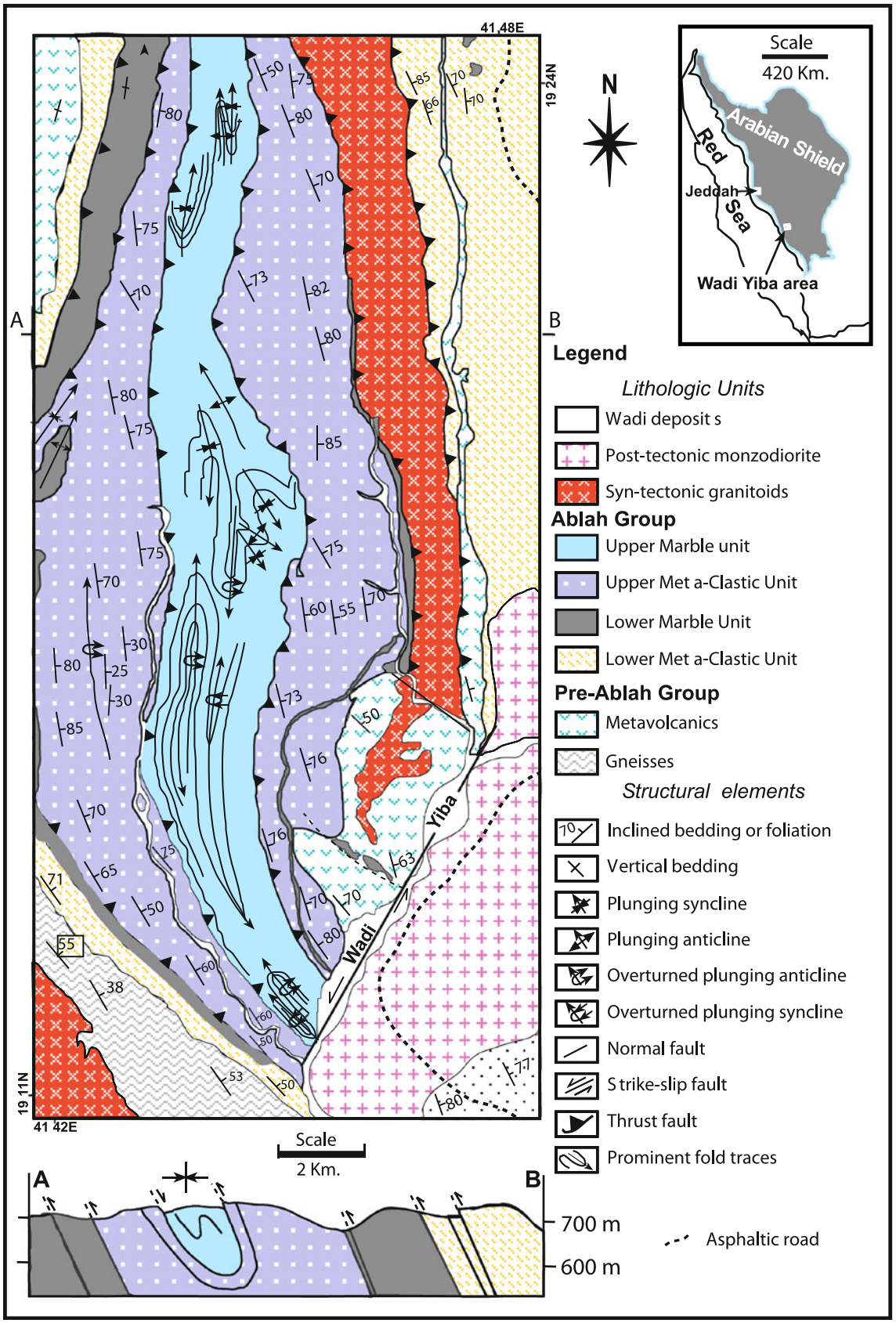

Fig. 1 Geologic map of Wadi Yiba area showing major structural elements

metaclastic unit are especially mylonitized and cataclased revealing tectonic contact between the gneiss and the lower part of Ablah Group. On the microscopic scale, these samples consist of plagioclase, K-feldspars and quartz porphyroclasts embedded in a fine-grained crushed matrix of the same components (Kattu 2011).

Metavolcanics

The metavolcanics are encountered northwest of Wadi Yiba, in addition to minor exposures in the extreme NW. Hornfels is prominent near the contact with the syn-tectonic granitoids. Some metavolcanics are compositionally metabasalts to metabasaltic andesites, consist of plagioclase and amphibole (mainly hornblende), together with micas, abundant opaques (magnetite and ilmenite), zircon and apatite. Other metavolcanics are rhyodacitic in composition, being composed of phenocrysts of sodium-rich plagioclase, K-feldspars, quartz, biotite and hornblende, embedded in fine grained crystalline matrix consisting of feldspars, quartz, biotite and opaques.

Ablah group

The type section of the Ablah Group (AG) is located in the southern Arabian Shield in the Ablah area (Bayley 1972). Rocks of this group are also found east and southeast of Al Aqiq town and at Wadi Yiba. In its type locality near Jabal Ablah, these rocks have been dated to 641±4 Ma using U-Pb method (Genna et al., 1999) and 613±7 Ma using U-Pb SHRIMP zircon method (Johnson et al. 2001). The metavolcanics and AG suffered low grade greenschist to low grade amphibolite facies metamorphism. Greenwood (1975) classified AG rocks in their type locality into three formations; Rafa'a, Jerub and Thurat Formations. Hadley (1975) subdivided AG at Wadi Yiba into two formations; Lower Saban and Upper Al-Hadb Formations.

AG in the study area comprises four main lithologic units; lower metaclastic-, lower marble-, middle metaclastic-, and upper marble-units (Fig. 2a). The lower metaclastic unit consists of beds 2 to 40 m thick of sandstone grading into siltstone, and is interpreted to be a deltaic deposit (Sanders et al. 1980). This unit has a basal conglomerate that contains matrix-supported cobbles of granite and pebbles of andesitic and rhyolitic lavas in a muddy micaceous, ankeritic matrix, with epidote and amphibole. Clasts are highly stretched parallel to the strike of the beds. A general thinning of this unit to the north suggests a source area in the southeast. The lower metaclastic unit is exposed in the eastern and western parts. Contacts with older metavolcanics and gneiss are tectonic rather than stratigraphic. Near the tectonic contact, the lower metaclastic unit is well foliated, lineated and isoclinally folded (Fig. 2b).

The lower marble consists of fine-grained siliceous carbonate interbedded with bands of chlorite schist, calcareous schist and quartz-biotite schist. It is well-bedded to massive, forming resistant, knife-edged ridges and well-developed folds. Petrographically, the lower marble has fine semi-phyllite and mosaic textures and contains rounded to sub-rounded sand grains. The rock is composed of calcite, with significant amount of quartz and mica. The upper metaclastic unit covers about 30 % of basement expsoures in the study

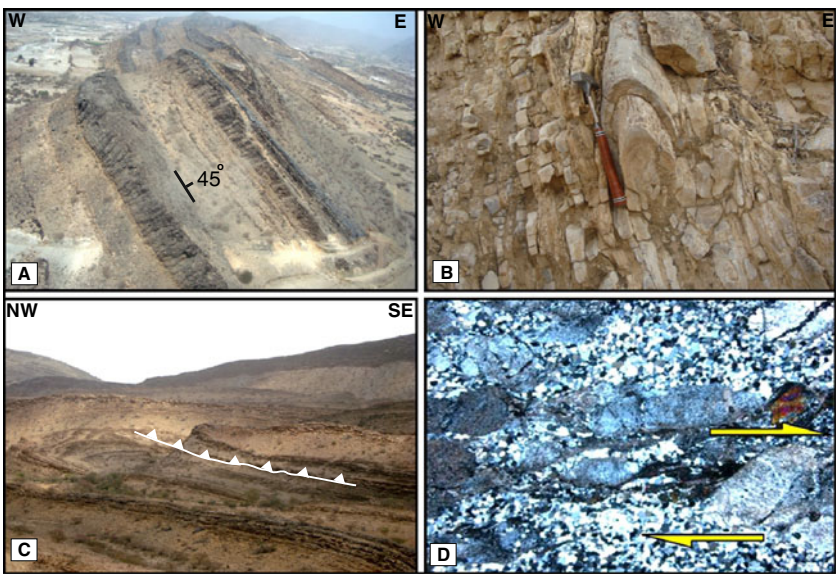

Fig. 2 Field photographs of AG metasediments and micrograph of syntectonic granitoid. **a** Black and yellow interlayers of lower marble unit showing eastward moderately inclined bedding (field of view ~70 m). **b** Isoclinal fold developed in the metamudstone of the lower metaclastic unit (hammer for a scale). **c** Alternating marble and metaclastic units showing isoclinal folds. Note the post-folding thrust; juxtaposition of two anticlinal closures due to thrust propagation (Width of view ~1 km). **d** Microphotograph of intensively deformed syn-tectonic granitoid with typical mylonitic texture. CN, 1.6X

area and shows evidence of rapid deposition. In the western part of the area, a typical succession consists of alternating metamorphosed shale, mudstone, sandstone, grit and conglomerate is encountered. These rocks are banded to laminated, foliated and folded. Coarser-grained beds form resistant ridges. In the north, the siltstone and mudstone are red to purple, suggesting deposition under oxidizing conditions in deltaic to continental environments. In the south, the rocks are gray to green in color, fine- to coarse-grained quartz-mica schists, meta-arkoses and metaconglomerates.

The upper marble unit occupies the central part of the study area (Fig. 1) and exhibits tectonic contact with the upper metaclastic unit. This unit is easily traced on the Landsat image. It shows spectacular map-scale tight overturned folds of different styles. It consists predominantly of buff to white color, fine-grained siliceous marble, analogous to that of the lower marble unit, intercalated with minor siltstone and sandy carbonate beds. A layer of black to gray, fine-grained argillaceous marble (up to 25 m thick) is persistent along strike for distances up to 22 km and shows remarkable isoclinal folds that have been cut by latter thrusts (Fig. 2c). On the microscope scale, the upper marble shows inequigranular mosaic texture and is wholly composed of calcite together with impurities of opaque minerals.

Granitoid rocks

One of the main interests of this study is to understand the nature of the contact between AG and plutonic rocks. In places, there is clear evidence that the granitoids were sheared (syn-tectonic), while in other places they appear to have intruded post-deformation.

Syn-tectonic granitoids

Syn-tectonic granitoids form an elongate N-S belt that extends for about 9 km from the northern border of the mapped area to the north of the main Wadi Yiba. These rocks display most of the essential features of syn-tectonic granitoids emplaced along shear zones and major thrusts in the ANS in order to accommodate W- to WSW-propagation and crustal relaxation; e.g. Abu-Beit mylonitized granite at Wadi Beitan area in the southern Eastern Desert of Egypt (Abdel-Khalek et al. 1992). The intrusion has apophyses that injected into all of the surrounding lithologic units (metavolcanics, lower- and upper-marble units, and upper metaclastic unit) revealing its intrusive nature. It is intensively cataclased and mylonitized (Fig. 2d), although it is often characterized by sheared outer margins and less deformed core. Syn-tectonic granitoids are composed of feldspar (mostly microcline and plagioclase) and quartz porphyroclasts set in a strongly cataclased groundmass of the same components together with hornblende and micas.

Post-tectonic monzodiorite

Post-tectonic monzogranite is the youngest Neoproterozoic lithology and is exposed in the southeastern sector of the map. It is coarse grained, buff to whitish gray in color, slightly fractured, weathered and undeformed. It has sharp intrusive contacts with AG lower metaclastic unit. It consists of 50 % plagioclase (calcic oligoclase), 28 %K-feldspars (orthoclase and microcline), and 22 % quartz, and a small percentage of micas (muscovite and biotite), secondary epidote and accessory opaques.

Structural pattern

The geometry and orientations of minor folds, bedding and foliation are generally consistent with the large N-S trending folds. The structures appear to have formed in a progressive two-stage sequence (D_1–D_2); early folding and foliation development during D_1 was followed by thrusting, shearing and the development of the Wadi Yiba Shear Zone (WYSZ) during D_2. D_3 represents the last deformation affecting the area and is characterized by F_3 open folds which overprint all earlier structures. AG marble member serves as marker for tracing large-scale folds (Fig. 1).

The study area is a part of a major fold-thrust belt affected by large-scale shearing. The exposed Neoproterozoic basement rocks display different types of planar and linear structural features of both primary and secondary origin. Primary structures commonly include bedding (Fig. 2a), cross-bedding and graded bedding in the slightly metamorphosed sedimentary rocks. These structures were used to determine younging direction and their relationships to subsequent structures. Secondary structures include folds, foliations, lineations, thrusts and shear zones.

D_1 deformation

Structures designated as D_1 include mesoscopic folds (F_1) and associated axial plane foliation (S_1) and mineral and stretching lineations (L_1), as well as boudinage structure. D_1 fabrics are pervasive throughout the study area and commonly show different styles in different deformed lithologies. They comprise small- and large-scale isoclinal (Fig. 2b, c) and intrafolial folds, here designated as F_1, found in the metavolcanics and the overlying AG. In some places of the mapped area, F_1 folds become upright and are locally westward verging. In other places, only tightly appressed folds and sheared out hinges are observed, and the attitudes of F_1 fold axes show variable orientations due to the effect of latter events. Because F_1 is reworked by subsequent D_2 and D_3 deformations, it is hard to restore F_1 to its original orientation. Parallel to the F_1 fold axial plane is S_1 that is usually a transposing and intrafolial foliations; S_1 surface is isoclinally folded and appear as fold hooks within other S_1 foliation reflecting a progressive transposition.

S_1 foliations mostly show a preferred orientation, although complex patterns of S_1 foliations are dominant in the central part of Wadi Yiba area due to later deformation. In the lithological layers enclosing the intrafolial folds, S_1 foliations are perceptibly parallel to bedding. On S_1 foliation planes, L_1 lineations are defined by preferred orientation of synkinematic minerals. Most of L_1 mineral and stretching lineations show variable orientations most probably due to the effect of the subsequent deformation phases. Boudinage related to D_1 deformation is sporadically distributed in the area, and boudins are co-axial to F_1 folds.

D_2 deformation

The tectonic regime prevailing during D_2 deformation phase was transpression which involves strike-slip shear accompanied by horizontal shortening and vertical lengthening in the shear plane (Sanderson and Marchini 1984; Dewey et al. 1998). Structures such as folds, tension fractures and Riedel shears are formed in the shear zones but at different angles to those in simple strike-slip faults. Structures associated with transpression in Wadi Yiba area include rodding lineations, mylonites, augen-structures and foliation fish. D_2 deformation is a progressive after D_1. Progressive deformation was involved in the generation of asymmetric folds (Fig. 3a). N- to NNW-oriented thrusts were formed during D_2. Thrust propagation formed F_2 thrust-related folds and occasional thrust duplexes (Fig. 3b). F_2 thrust-related folds are frequently overturned, with gentle eastern limbs and steep western overturned limbs (Fig. 3c).

Mesoscopic and microscopic shear sense indicators reveal that D_2 shearing was dextral (Fig. 3d, e). The main WYSZ and other small unmappable shear zones formed due to this shearing. Dextral transpression is consistent with the mega-scale sigmoidal pattern observed on the Landsat image (Fig. 4) and led to the formation of F_2 shear zone-related folds.

D_3 deformation

D_3 deformation is manifested by F_3 folds, S_3 axial plane foliations and L_3 crenulation lineations and kink bands, overprinting older

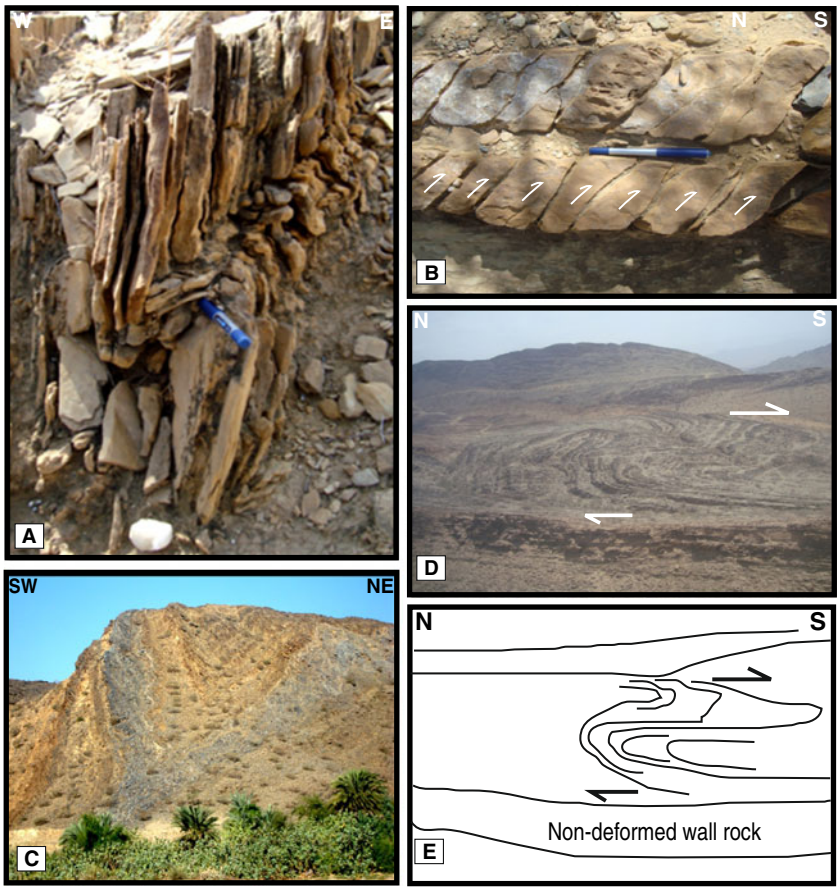

Fig. 3 Field photographs of AG showing folding, thrusting and shearing. **a** S-shaped fold of the D_2 deformation, useful in vergence analysis to locate large-scale antiforms and synforms. **b** Remarkable internal imbrications and duplexing of a single marble layer (pen for a scale). **c** F_2 synformal thrust-related fold, with gentle eastern limb and steep western limb. Northwestern flank of Wadi Yiba (field of view~60 m). **d** Large-scale dextral shearing cutting across pre-existing folds. Sheared folds are observed at the margins of the shear zone, while inside it, folds are completely transposed (width of view ~0.5 Km). **e** Traced sketch showing features in (**d**)

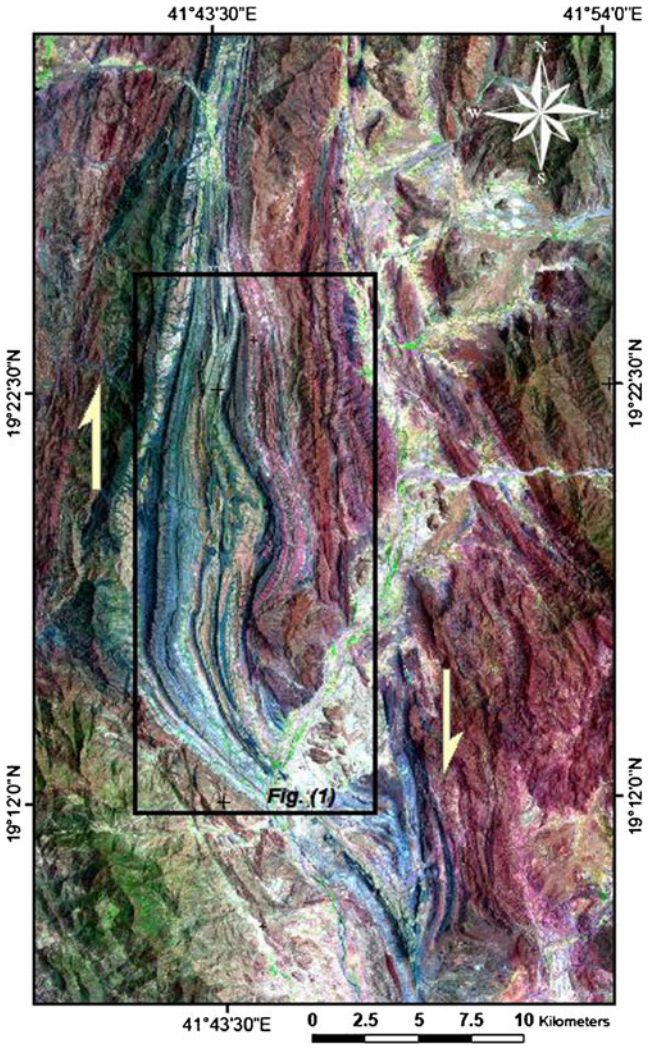

Fig. 4 A Landsat ETM^{+} FCC image (R7, G4, B2) of Wadi Yiba area showing well-developed maga-scale sigmoidal pattern interpreted with dextral sense of shear

fabrics (Fig. 5a, b). F_3 folds are frequently open and have steep to subvertical axial planes and axes that plunge moderately to steeply towards the E, ENE and ESE. Whereas F_1 and F_2 folds are coaxial and steeply to moderately N plunging (Fig. 5c, d), F_3 folds trend roughly E-W; i.e. perpendicular to F_1 and F_2 (Fig. 5e, f). L_3 crenulation lineations and kink bands formed only in rocks containing pre-existing, well-developed foliations and those with uniform layer thickness (Anderson 1964; Weiss 1980). L_3 crenulation lineations and kink bands deform S_2 and are particularly common in the AG metasediments. D_3 deformation has rotated S_2 foliations from N-S trends to E, ENE and ESE trends.

Geometrical analysis

In the study area, planar structures are represented by foliation planes, whereas linear structures encompass fold hinges, mineral lineations, stretching lineations, crenulation lineations, kink bands, intersection lineations and boudinage. The planar and linear structural elements are used to build a model of the macroscopic structures of the area. Conventional geometrical analysis was carried out on the poles of planar structures and plunge of lineations of mesoscopic structural elements on lower hemisphere equal area stereonet (Schmidt net). Geometric interpretation of the data was done by inspection, assisted by contouring methods to predict the geometry of the larger structures that are difficult to resolve by standard field methods. Collected measurements are plotted and contoured using "*Spheristat v. 2.2*" Software Program.

S-surfaces (Foliations/Bedding)

A total of 123 orientation measurements of S surfaces (bedding and foliations) were taken. S_1 foliations trend NW and have moderate to steep dips (30–80°) mainly NE. Poles to S_1 from the main outcrops show a girdle distribution (Fig. 6a), which is interpreted to indicate folding about an axis plunging 70° to the NE (Fig. 6b). Inspection of the diagram (Fig. 6b) reveals that poles to S_1-surfaces are distributed along two great circles indicating at least two folding phases. The first great circle strikes 090° and dips 83°S; its pole plunges 17° towards the N. The second girdle of poles strikes 172° and dips 25° WSW, with girdle pole (65° towards 082°). Based on field observations and presence of type-3 fold interference pattern, it is concluded that F_1 and F_2 folds are coaxial.

Lineations

Lineations include mineral and stretching lineations and the hinges of minor folds. These linear structures trend due N with a moderate to steep plunge (30–85°) and toward the NE with a moderate plunge (40–50°) (Fig. 6c). The stereogram shows two data concentrations (Fig. 6d). The first concentration plunges 46° on a bearing 350° and was associated with F_1 and F_2 folds. The second data concentration plunges 63° on a bearing 058° and is related to the F_3 folding generation.

Discussion and tectonic evolution

Neoproterozoic basement in the Wadi Yiba area were deformed after AG metasediments were deposited about 615–640, about the time that collision between major fragments of East and West Gondwana fragments estimated to have begun ~630 Ma. This deformation records the evolving strain field as convergence continued for the next ~40 million years.

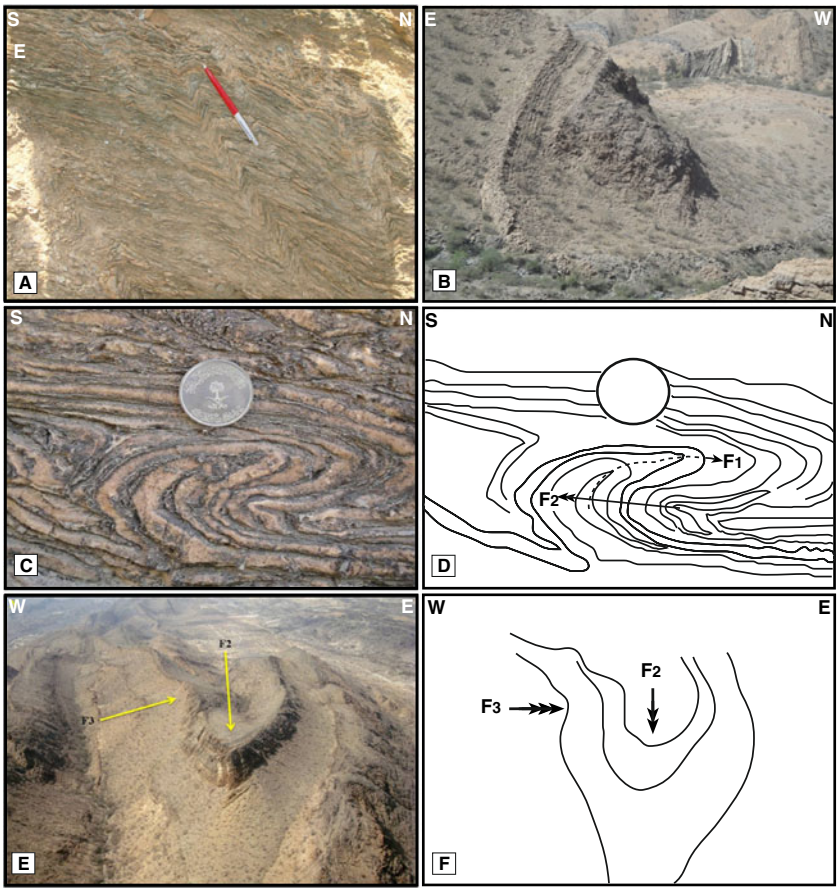

Fig. 5 Field photographs showing D_1, D_2 and D_3 structures. **a** Asymmetric crenulation foliation "S_3" developed in the upper metaclastic unit, overprinting early formed fabrics. **b** Open fold developed in interlayered marble and metsclastic units (width of view ~35 m). **c** F_1 isoclinal fold refolded by F_2 fold, upper marble unit. Note F_1 and F_2 are coaxial. **d** Sketch illustrating features in (**c**). **e** F_1 isoclinal fold and F_2 overturned fold superposed by F_3 open fold, Upper marble unit (Width of view ~2.0 Km). **f** Sketch showing features in (**e**)

Folding, thrusting and shearing relations

The structural style and sequence of overprinting within high strain zones provide key kinematic and displacement information which can constrain the relative timing of tectonic transport and deformation, as well as information regarding crustal reactivation and reworking (Butler et al. 2006; Stewart et al. 2009). In the Wadi Yiba area, folding and thrusting, as well as transcurrent shearing are geometrically and kinematically related as in many areas in the ANS; e.g. El-Sibai Core Complex (Abdelwahed, 2008), Beitan (Abdel-Khalek et al. 1992) and Urf Umm Araka (Hamimi 2000) in the Egyptian Nubian Shield, and Ad-Damm (Matsah et al. 2004) and Al-Jammom (Matsah et al. 2005) in Saudi Arabian Shield.

Thrust-related folds

The thrusts in the study area were propagated sequentially in an "in-sequence" styles according to footwall-nucleating-footwall vergent rule, where earlier hangingwalls are carried forwards in a piggyback manner, and each new thrust developed in the footwall of the previous thrust. Opposite thrusts, pop-up structures and out-of-sequence thrusts are rarely recognized. Out-of-sequence thrusts form behind the principal thrusts, and therefore are not parts of the foreland- propagating sequence. In many exposures, particularly in AG marble units, arrays of thrust horses bounded by floor thrusts (i.e. sole thrusts) at the base and by roof thrusts at the top are encountered, forming thrust duplex structures. The stacking of horses and hence duplex shapes depends on ramp angle, thrust spacing and displacement on individual link thrusts. Observable duplexes range from centimeters (Fig. 3b) to meters in scale. Duplexes in the study area were used as indicators of shortening and contraction. The progressive development and propagation of ~600 Ma thrust faults and thrust duplexes in the Neoproterozoic rocks exposed in the area caused F_2 thrust-related folds.

Shear zone-related folds

Shear zones cut across and run roughly parallel to the D_1 and D_2 folded AG rocks. Final fold geometry was modified by transcurrent shearing and so depends mainly on the

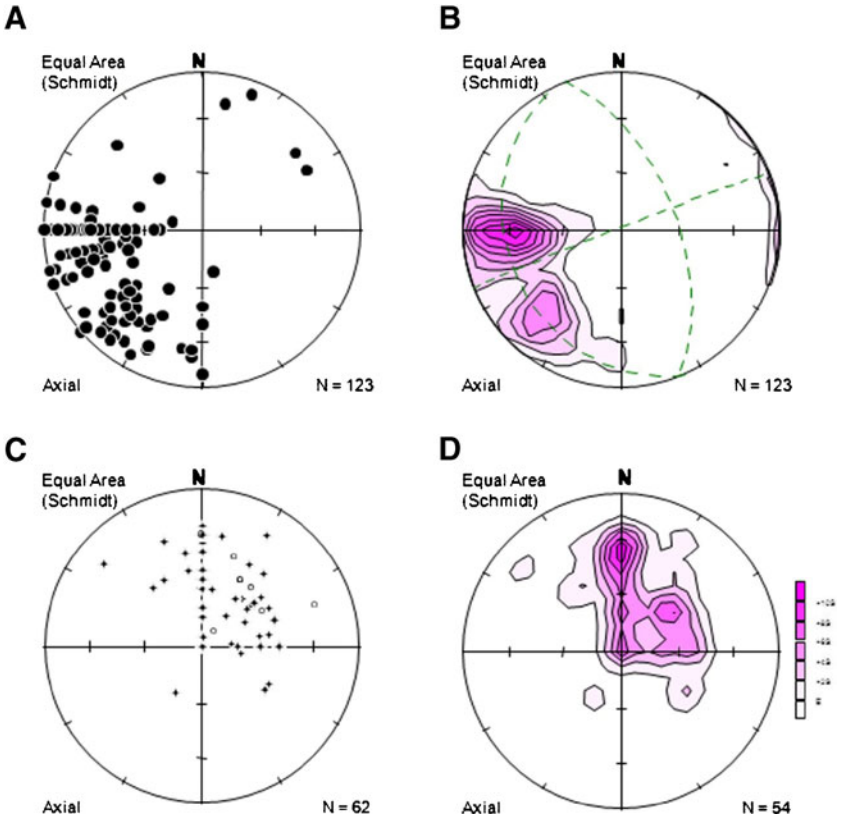

Fig. 6 Orientational data (lower hemisphere equal area projections): **a**, **b** pole diagram and its contour equivalents of 123 bedding and foliation planes measured throughout the entire area. **c** point diagram of 62 small fold hinges (crosses) and mineral lineations (*circles*). **d** contour diagram of 54 fold hinges. NE, N and NW trending hinges are related to F_1 and F_2 generations, whereas the eastern most trending folds belong to F_3 generation

rheology and the initial orientation of the folded surface relative to the kinematic framework. These folds were transposed and deflected by transcurrent shearing (Fig. 3d). On the other hand, the overprinting relationships between thrust-related folds and shear zone-related folds recorded in many exposures in the mapped area, especially in the highly strained WYSZ, indicates that thrust-related folds were overprinted by the shear zone-related folds. Remarkable dextral shearing overprinted thrust-related folds (Fig. 4). The presence of oblique stretching lineations and tension gashes (Fig. 7a) along thrust planes are also evidence that thrusting predated transcurrent shearing (Fig. 7b). Although WYSZ exhibits a complete transition from slightly sheared or even unsheared to highly strained rocks, deciphering such relationships between folding and both thrusting and transcurrent shearing could be detected easily throughout the mapped area.

Structural succession

Field-structural mapping reveals that the Wadi Yiba area experienced at least three phases of deformation (D_1–D_3.).

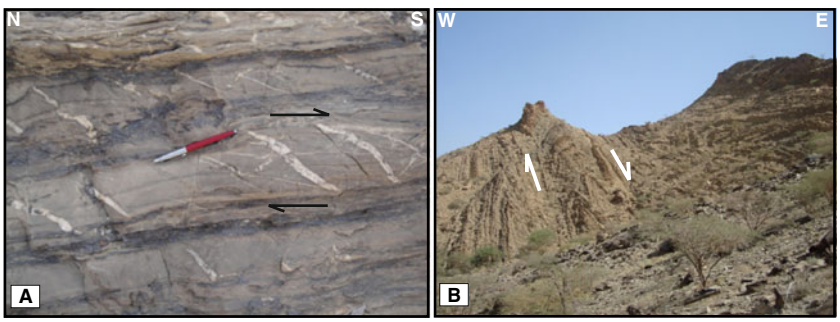

Fig. 7 Meso-scale shear-related structures. **a** Dextral en-echelon tension gashes of quartz veins in upper marble unit. **b** F_2- shear zone-related folds in upper marble unit (width of view ~50 m)

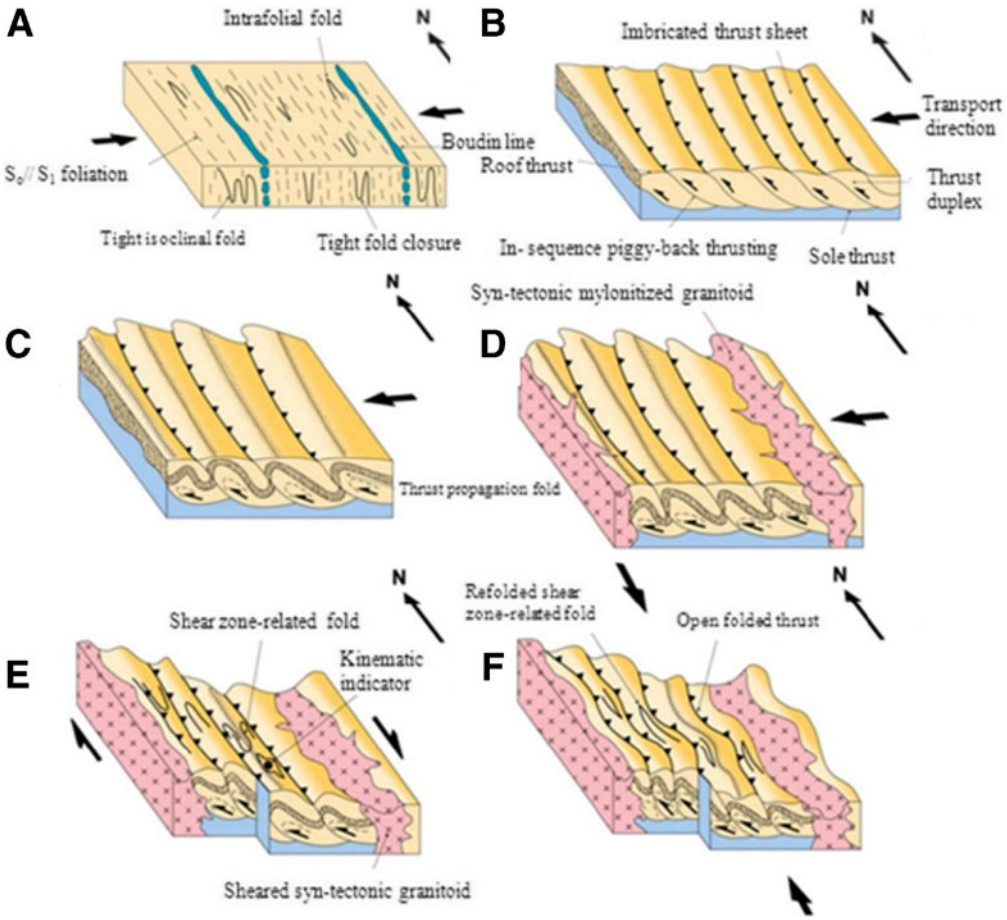

Fig. 8 Three-dimensional cartoon illustrating a preferred sequence of tectonic events in Wadi Yiba area, Western Arabian Shield, Saudi Arabia. **a** Initial E-W (to ENE-WSW) shortening and development of D_1 Structures. **b** W- (to WSW-) propagating thrusting and evolution of thrusting into transpression during D_2. **c** Formation of thrust-related overturned folds. **d** Emplacement and exhumation of syn-tectonic granitoid in order to accommodate W- to WSW-propagation and crustal relaxation. **e** Dextral shearing and formation of the WYSZ and minor shears. **f** N-S (to NNE-WSW) shortening and formation of D_3 structures

The structural relations and sequence of tectonic events are simplified and illustrated in three- dimensional block diagrams (Fig. 8). D_1 is interpreted as due to early E-W (to ENE-WSW) shortening as collision began between East and West Gondwana ~630 Ma. D_1 was the main folding phase and formed tight isoclinal and intrafolial folds in the metavolcanics and overlying AG metasediments (Fig. 8a). These folds are clearly visible at multiple scales. Megascopically (whole area), F_1 and F_2 folds display a series of antiformal and synformal structures with axes oriented roughly N-S (Fig. 1). Folding was accompanied by development of a pervasive foliation roughly parallel to the axial plane of mesoscopic folds. In some places, F_1 folds are upright and locally westward verging. In other places, F_1 folds verge to the W, though they have upright axial planes. Boudinage related to D_1 deformation is sporadically distributed in the area, and is co-axial with F_1 fold axes, indicating the stretching of bedding perpendicular to F_1 axes (e.g. Fossen 2010).

Shortening evolved into transpression during D_2, which is a progressive stage of D_1. N- to NNW-trending thrusts formed during D_2 (Fig. 8b) Thrust propagation occurred according to the "footwall-nucleating-footwall-vergent rule" where younger thrusts initiated in the footwalls of the older one as in many areas in the ANS. Thrust propagation formed F_2 thrust-propagation folds (Fig. 8c) and occasional thrust duplexes. F_2 thrust-related folds are frequently overturned, with gentle eastern limbs and steep westward-overturned limbs.

Field relations in the Wadi Yiba area strongly support the idea that the syn-tectonic granitoids were emplaced during D_2 transpression (Fig. 8d). The intensive degree of shearing and mylonitization reveal that granitoids were emplaced into space generated by thrust propagation. Similar relation was described in N-trending Nabitah and Hanabiq dextral shear zones (e.g. Genna et al. 2002; Duncan et al. 1990; Johnson et al. 2011).

W- to WSW-transport direction is proposed based on stretching lineation trajectories, S-C foliations, asymmetric

shear fabrics and related mylonitic foliation, flat-ramp and duplex geometries. The N- to NNW- orientation of both thrusts and axial planes of minor and major F_2 thrust-related overturned folds supports the same stress trajectories of compressional regime during the D_2 deformational phase and a W- to WSW-propagation of thrusting in the study area. Mesoscopic and microscopic shear sense indicators on the associated D_2 strike-slip shear zones (e.g. the WYSZ and smaller shears) reveal that shearing was dextral (Fig. 8e). Dextral shearing is also consistent with the mega-scale sigmoidal pattern seen on the Landsat image (Fig. 4). The WYSZ is similar to other brittle-ductile N-S-trending Late Neoproterozoic shear zones found in the southern ANS (Abdelsalam and Stern 1997). D_1 and D_2 structures are locally overprinted by D_3 structures (F_3 open folds, S_3 axial plane foliations and L_3 crenulation lineations and kink bands). D_3 is interpreted as due to N-S to NNW-SSE shortening (Fig. 8f). F_3 folds are commonly open and have steep to subvertical axial planes and axes plunge moderately to steeply towards the E, ENE and ESE .

Concluding remarks

The main conclusions emerging from studying the Neoproterozoic basement exposed in the Wadi Yiba area in the southern Arabian Shield, Saudi Arabia are summarized as follows:

1) Basement lithologies consist mainly of gneisses, metavolcanics, ~620–640 Ma AG metasediments and syn- and post-tectonic granitoids.
2) AG comprises metaclastic and marble units, which records deformation well.
3) Structures evolved during three phases of deformation (D_1, D_2 and D_3).
4) D_1 is interpreted as due to early E-W (to ENE-WSW) shortening as collision began between East and West Gondwana ~630 Ma.
5) D_2 reflects heterogeneous transcurrent shear during dextral transpression and was particularly important in the structural shaping of the region. It generated the most conspicuous structural element in the area (identified for the first time as the WYSZ), including F_2 thrust- and shear zone- related folds.
6) Mesoscopic and microscopic kinematic indicators indicate dextral sense of shear. This shearing sense is consistent with the mega-scale sigmoidal pattern clearly recognizable on Landsat image; i.e. this structural pattern is penetrative throughout the mapped area and environs.
7) N-S trending brittle-ductile late Neoproterozoic shear zones in the ANS as typified WYSZ reflect concentration of transpressive strain accompanying collisional shortening beginning ~630 Ma.

Acknowledgments The Saudi Geological Survey and Faculty of Earth Sciences, King Abdulaziz University are acknowledged for providing us a logistic support during a thirty-day field program (April-May, 2010). Fruitful discussion with Profs. S. Khawasik, P.R. Johnson, M. Abdelwahed and Y. El-Kazzaz are gratefully acknowledged. Dr. A. Elfakharani is thanked for supportive review. We thank and appreciate the two anonymous reviewers for their distinguished comments and suggestions that greatly improved the manuscript.

References

Abdeen MM, Abdelghaffar AA (2011) Syn- and post-accretionary structures in the Neoproterozoic Central Allaqi-Heiani Suture Zone, Southeastern Egypt. Precambrian Res 185:95–108

Abdel-Khalek ML, Takla MA, Sehim A, Hamimi Z, El Manawi AW (1992) Geology and tectonic evolution of Wadi Beitan area, south Eastern Desert, Egypt. GAW Cairo Univ 1:369–393

Abdel-Khalek ML, Takla MA, Sehim A, Abdel Wahed M, Hamimi Z, Sakran Sh (1999) Geology and tectonic evolution of the shield rocks, east Wadi Beitan area, south Eastern Desert, Egypt. Egypt J Geol 43(1):1–15

Abdelsalam MG, Stern RJ (1997) Sutures and Shear Zones in the Arabian-Nubian Shield. J Afr Earth Sci 23:289–310

Abdelsalam MG, Abdeen MM, Dowidar HM, Stern RJ, Abdelghaffar AA (2003a) Evolution of the Neoproterozoic Allaqi-Heiani Suture Zone, southern Egypt. Precambrian Res 124:87–104

Abdelsalam MG, Abdel-Rahman ESM, El-Faki EFM, Al-Hur B, El-Bashier FRM, Stern RJ, Thurmond AK (2003b) Neoproterozoic deformation in the northeastern part of the Saharan Metacraton, northern Sudan. Precambrian Res 123:203–221

Abdelwahed MA (2008) Thrusting and transpressional shearing in the Pan-African nappe southwest El-Sibai Core Complex, Central Eastern Desert, Egypt. J Afr Earth Sci 50:16–36

Akaad MK, Noweir AM (1980) Geology and lithostratigraphy of the Arabian Desert orogenic belt of Egypt between latitudes 25° 35′ S and 26° 30′ N. Inst Appl Geol Jeddah Bull 3:127–135

Anderson TB (1964) Kink-bands and related geological structures. Nature 202:272–274

Bayley RW (1972) Geological map and section of Wadi Yiba quadrangle [19/41D]: Saudi Arabian Directorate General of Mineral Resources Geologic Map GM-1, Scale 1:100.000, with text, 6 p

Butler R, Tavarnelli E, Grasso M (2006) Structural inheritance in mountain belts: an Alpine–Apennine perspective. J Struct Geol 28:1–16

Dewey JF, Holdsworth RE, Strachan RA (1998) Transpression and transtension zones. In: Hodsworth RE, Strachan RA, Dewey JF (eds.), Continental Transpressional and Transtensional Tectonics, Special Publ 135, Geol Soc London 1–14.

Duncan IJ, Rivard B, Arvidson RE, Sultan M (1990) Structural interpretation and tectonic evolution of a part of the Najd Shear Zone (Saudi Arabia) using Landsat thematic-mapper data. Tectonophysics 178:309–315

El-Amawy MA, Said M, El Alfy ZS, Allah MA (2000a) Geology and tectonic evolution of Wadi Madi area, south Eastern Desert, Egypt. Ann Geol Surv Egypt 23:15–32

El-Amawy MA, Wetait MA, El Alfy ZS, Shweel AS (2000b) Geology, geochemistry and structural evolution of Wadi Beida area, south Eastern Desert, Egypt. Egypt J Geol 44(1):65–84

El-Amawy M, Hamimi Z, Dardir W (2001) Structural analysis of Gabal El- Gerf and environs, south Eastern Desert, Egypt: evidence of frontal and oblique thrusting. Geol Africa Assiut Univ 2(2):99–116

El-Gaby S, List FK, Tehrani R (1988) Geology, evolution and metallogenesis of the Pan-African belt in Egypt. In: El-Gaby S, Greiling RO (eds) The Pan-African Belt of Northeast Africa and adjacent

areas: tectonic evolution and economic aspects of a late proterozoic Orogen. Vieweg and Sohn, Braunschweig, Wiesbaden, Germany, pp 17–65
Fossen H (2010) Structural geology. Cambridge University Press, London, 457 p
Genna A, Guerrot C, Deschamps Y, Nehlig P, Shanti M (1999) Les formations Ablah d'Arabie Saoudite (datation et implication géologique). Compte Rendue Acadamie Sciences, Paris 329:661–667
Genna A, Nehlig P, Le Goff E, Guetrrot C, Shanti M (2002) Proterozoic tectonism of the Arabian Shield. Precambrian Res 117:21–40
Greenwood WR (1975) Geological map of the Jabal Ibrahim quadrangle [20/4C]: Saudi Arabia Directorate General of Mineral Resources Geologic Map GM22
Hadley DG (1975) Geological map of the Qunfudah quadrangle [19/19C]: Saudi Arabian directorate general of mineral resources geologic Map 6M-91. Scale 1:100.000
Hamimi Z (1996) Tectonic evolution of the shield rocks of Gabal El-Sibai area, central Eastern Desert, Egypt. Egypt J Geol 40(1):423–453
Hamimi Z (2000) Thrust duplex system in Urf Um Araka area, south Eastern Desert, Egypt. Egypt J Geol 44(2):19–29
Hamimi Z, El-Kazzaz Y (2000) Fold geometry and folding mechanism in Um Krush Klippe, south Eastern Desert, Egypt. GAW Cairo Univ 5:605–618
Hamimi Z, El-Amawy MA, Wetait M (1994) Geology and structural evolution of El-Shalul dome and environs, Central Eastern Desert of Egypt. Egypt J Geol 38:575–595
Jacobs J, Thomas RJ (2004) Himalayan-type indenter-escape tectonics model for the southern part of the late Neoproterozoic–early Paleozoic East African–Antarctic Orogen. Geology 32:721–724
Johnson PR (1998) The structural geology of the Samran-Shayban area, Kingdom of Saudi Arabia: Saudi Arabian Deputy Ministry for Mineral Resources Open File Report USGS-OF-98-2, 45p
Johnson P, Woldehaimanot B (2003) Development of the Arabian-Nubian Shield: perspectives on accretion and deformation in the northern East African Orogen and the assembly of Gondwana. In: Yoshida M, Windley BF, Dasgupta S (eds) Proterozoic East Gondwana: Supercontinent Assembly and Breakup. Geol Soc London Special Publ 206:290–325
Johnson PR, Kattan FH, Wooden JL (2001) Implications of SHRIMP and microstructural data on the age and kinematics of shearing in the Asir terrane, southern Arabian Shield, Saudi Arabia. Gondwana Res 4:172–173
Johnson PR, Andresen A, Collins AS, Fowler AR, Fritz H, Ghebreab W, Kusky T, Stern RJ (2011) Late Cryogenian–Ediacaran history of the Arabian–Nubian Shield: A review of depositional, plutonic, structural, and tectonic events in the closing stages of the northern East African Orogen. J Afr Earth Sci 61:167–232
Kattu G (2011) Structural Evolution of Wadi Yiba area, southern Arabian Shield, Saudi Arabia. Unpublished M.Sc. Thesis, Faculty of Earth Sciences, King Abdulaziz Univ., Saudi Arabia. 141p
Liégeois JP, Stern RJ (2010) Sr-Nd isotopes and geochemistry of granite-gneiss complexes from the Meatiq and Hafafit domes, Eastern Desert, Egypt: No evidence for pre-Neoproterozoic crust. J Afr Earth Sci 57:31–40
Matsah MI, Qari MHT, Hegazi AM, Amlas MA, Hamimi Z (2004) The Neoproterozoic Ad-Damm shear zone: dextral transpression in the Arabian Shield, Saudi Arabia. Egypt J Geol 48:215–236
Matsah MI, Qari MHT, Hegazi AM, Amlas MA, Hamimi Z (2005) Kinematics and progressive deformational history of Al-Jamoom Pan-African belt, Western Arabian Shield, Saudi Arabia. Ann Geol Surv Egypt XXVIII:111–131
Muhongo S, Hauzenberger C, Sommer H (2003) Vestiges of the Mesoproterozoic events in the Neoproterozoic Mozambique belt: the East African perspective in the Rodinia puzzle. Gondwana Res 6(3):409–416
Patchett PJ, Chase CG (2002) Role of transform continental margins in major crustal growth episodes. Geology 30:39–42
Sanders RN, Tedder IJ, Ford CR, Circosts G (1980) Stratiform copper search in the southern Ablah group, Kingdom of Saudi Arabia: Utah Saudi Arabian Inc. unpublished report no
Sanderson D, Marchini RO (1984) Transpression. J Struct Geol 6:449–458
Sengör AMC, Natal'in BA (1996) Turkic-type Orogeny and its role in the making of the continental crust. Ann Rev Earth Planet Sci 24:263–337
Shackleton RM (1986) Precambrian collision tectonics in Africa. Geol Soc Special Publ 19:329–349
Shackleton RM (1994) Review of Late Proterozoic sutures, ophiolitic melanges and tectonics of eastern Egypt and north-east Sudan. Geol Rundshau 83:537–546
Shackleton RM (1996) The final collision zone between East and West Gondwana: Where is it? J Afr Earth Sci 23:271–287
Stein M, Goldstein SL (1996) From plume head to continental lithosphere in the Arabian-Nubian Shield. Nature 382:773–778
Stern RJ (1994) Arc assembly and continental collision in the Neoproterozoic East African Orogen: Implications for the consolidation of Gondwanaland. Ann Rev Earth Planet Sci 22:319–351
Stern RJ (2002) Crustal evolution in the East African Orogen: A neodymium isotopic perspective. J Afr Earth Sci 34:109–117
Stern RJ, Abdelsalam MG (1998) Formation of juvenile continental crust in the Arabian-Nubian Shield: Evidence from granitic rocks of the Nakasib suture, NE Sudan. Geol Rundshau 87:150–160
Stern RJ, Johnson PR (2010) Continental lithosphere of the Arabian Plate: A geologic, petrologic, and geophysical synthesis. Earth Sci Rev 101:29–67
Stern RJ, Johnson PR, Kröner A, Yibas B (2004) Neoproterozoic ophiolites of the Arabian-Nubian Shield. In: Kusky T (ed) Precambrian ophiolites. Elsevier, Amsterdam, pp 95–128
Stewart JR, Betts PG, Collins AS, Schaefer BF (2009) Multi-scale analysis of Proterozoic shear zones: An integrated structural and geophysical study. J Struct Geol 31:1238–1254
Stoeser DB, Camp VE (1985) Pan-African microplate accretion of the Arabian Shield. Geol Soc Am Bull 96:817–826
Vail JR (1985) Pan-African (late Precambrian) tectonic terrains and the reconstruction of the Arabian-Nubian Shield. Geology 13:839–842
Weiss LE (1980) Nucleation and growth of kink bands. Tectonophysics 65:1–38